QCD parton recombination and applications to nuclear structure functions

Frank E. Close
Oak Ridge National Laboratory, Oak Ridge, Tennessee 37831
and Physics Department, University of Tennessee, Knoxville, Tennessee 37996

Jianwei Qiu
High Energy Physics Division, Argonne National Laboratory, Argonne, Illinois 60439

R. G. Roberts
Rutherford Appleton Laboratory, Chilton, Didcot, OXON OX11 OQX, England
(Received 20 March 1989)

We investigate a hitherto neglected sector of perturbative QCD which is normally hidden in conventional hadron analyses but has observable consequences in nuclei. There is a modification to structure functions arising from the *fusion* of quarks, antiquarks, and gluons and we derive recombination factors, analogues of familiar splitting functions, and compute the effects of parton fusion on the nuclear structure functions. This mechanism causes the structure functions to extend beyond $x=1$; as $x\to 0$ we have a source of shadowing within the framework of QCD. We find that the loss of momentum when nucleons bind is shared almost equally between $q\bar{q}$ and gluons. We predict that the nuclear modification of the gluon distribution is a significant suppression as $x\to 0$ and enhancement for $x\simeq 0.2$. We point out how hadronic ψ production may be used to disentangle this shadowing mechanism from other nuclear effects.

I. INTRODUCTION

In perturbative QCD the evolution of the parton distributions is controlled by splitting functions where quarks or antiquarks radiate gluons, or where gluons convert into quark-antiquark pairs. Quarks and gluons can also fuse together [Fig. 1(b) contrast Fig. 1(a)]. Although these "fusion" diagrams are necessary contributions in a complete theory, they do not usually appear explicitly in the literature; instead their effects are subsumed within the input parton distributions [see e.g., Fig. 1(c)].

However, there are circumstances where fusion topologies can play an explicit role. When several nucleons are in close proximity (as in a nucleus, for example) a parton from one nucleon could leak into a neighbor and fuse with one of the latter's partons. The perturbation diagrams arising from such fusions and which "connect" partons of two or more nucleons will give to a collection of juxtaposed nucleons properties that the individual isolated nucleons would not possess.

While this leakage can occur for all partons, the most important contributions arise from partons with the largest spatial uncertainty, i.e., those significant as $x\to 0$. The effect of gluon fusion is expected to be appreciable at small x where the gluon density will be dramatically suppressed. At the same time the small-x behavior of the quarks is largely governed by the gluon density and so the shadowing of the gluons is translated into a shadowing of the nuclear structure function. Until now, discussion of this effect has concentrated on the Q^2 dependence only,[1,2] leading to a modified form of the Altarelli-Parisi equations, the x dependence of the gluon shadowing having been assumed.[3] One of the results of this paper is the derivation of the shape of this shadowing. Another interesting situation occurs when an exchanged wee gluon is absorbed by a hard quark in the neighbor nucleon, thereby boosting the quark to a larger value of x, even to $x>1$. Thus modifications to $F_2(x)$ at any x can occur from this mechanism. To the extent that this naturally

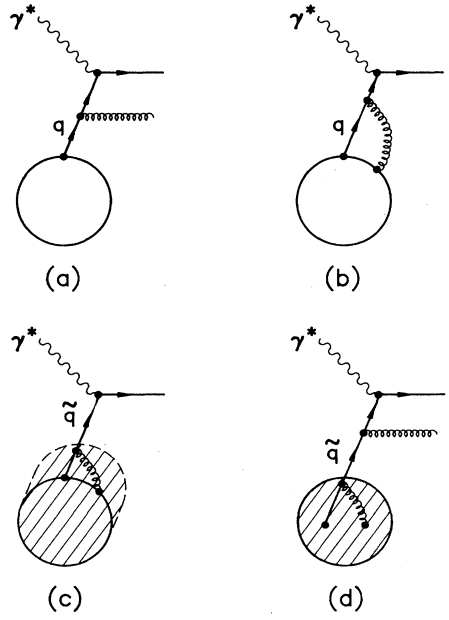

FIG. 1. (a) Gluon radiation from quark q at $O(\alpha_s)$; (b) fusion of quark q and gluon g at $O(\alpha_s)$; (c) qg fusion of (b) subsumed in quark input distribution $\bar{q}$ which is then evolved (d).

causes $F_2(x>1)\neq 0$ we have a QCD description of effects which are well known in nuclear physics. In this paper we develop and apply a formalism for the fusion of quarks, antiquarks, or gluons at all x.

In Sec. II we develop the formalism for qg, gg, and $q\bar{q}$ fusion. This technology reveals a pleasing simplicity in the resulting expressions, which are similar to the Altarelli-Parisi splitting functions but with difference of detail due to $2\rightarrow 1$ as against $1\rightarrow 2$ phase space and flux factors. For the first time we have a derivation of the recombination factor guessed at in some earlier literature[4] in the context of hadronic collisions.

In Sec. III we apply these techniques and obtain the modifications to $q^{N_1}(x)$, $\bar{q}^{N_1}(x)$, and $g^{N_1}(x)$ that arise when nucleon N_1 is in the vicinity of another nucleon, N_2, whose wee partons can leak out and fuse with those in N_1 (and vice versa). The results are easy to understand. In the vicinity of $x\rightarrow 1$ ($x\geq 0.5$), $q^N(x)$ falls rapidly with x and the absorption of a wee gluon tends on the average to increase the probability of finding fast quarks. Furthermore, it removes a slow quark $[q(x)\rightarrow q(x+\delta x)]$. In addition one has to allow for quarks being annihilated by exchanged antiquarks. The net effect is that wee quarks ($x\lesssim 0.2$) are reduced and quarks with $x\gtrsim 0.2$ are enhanced in probability.

Similar effects are found for gluons. Soft gluons are reduced due to absorbtion by q, $\bar{q}$, or gluons. In the latter case a gluon appears in the final state, courtesy of the g^3 vertex, with boosted momentum. Again, as for quarks, the tendency is for wee gluons to be depleted and for hard gluons to be enhanced relative to the initial distributions in free nucleons.

In this paper we consider a particular mechanism: namely, the fusion of evolved partons from different nucleons in the nuclear target for a particular process, namely, deep-inelastic scattering of leptons off a nucleus. While this is certainly not the main mechanism for nonadditive nuclear effects over the entire x range, it could well be the dominant ingredient in modifying the structure function at low x (by generating shadowing[1,3]) and at large x. It would be logically consistent to combine this mechanism with Q^2 rescaling[5] [which successfully describes the European Muon Collaboration (EMC) effect for intermediate x] to complete a QCD-based description of effective nuclear structure functions in terms of short-distance quark and gluon interactions. Nonadditive nuclear effects occur in other processes such as exclusive hadronic reactions and elastic lepton-hadron scattering where a knowledge of the bound-state wave function is necessary. Such processes are not studied here. One other situation, however, where the fusion of gluons should play a role is in the hadronic inclusive production of J/ψ. Despite the fact that the $gg\rightarrow c\bar{c}$ subprocess may also be suppressed by interactions between the c and $\bar{c}$ and the nuclear medium, we propose a method of disentangling the two effects and thereby expose the gluon shadowing mechanism. In the main, the aim of this paper is to investigate parton recombination in the nucleus within the context of deep-inelastic scattering and to understand the qualitative consequences.

II. DEFINITIONS AND FORMULAS

In this section we develop consistent definitions of parton number densities and derive the formulas for parton-parton fusion (e.g., qg, gg, and $q\bar{q}$). We shall show that these fusion processes manifestly alter the parton number densities, are self-consistent components of parton evolution, and preserve all kinematical constraints such as momentum conservation and valence-quark number conservation. The resulting expressions are similar to the Altarelli-Parisi splitting functions but with differences of detail due to $2\rightarrow 1$ as against $1\rightarrow 2$ phase space and flux factors.

We define the parton number densities through deep-inelastic lepton-hadron scattering. (In this paper we shall discuss only the leading tree-diagram fusion contributions and so are not affected by renormalization- and factorization-scheme dependence of the parton number density definitions.) First we introduce an auxiliary light-like vector n to fix the gauge as $n\cdot A=0$, where A is the gluon field. In the parton model, we define the cross section of a virtual photon off a hadron as shown in Fig. 2:

$$d\sigma(\gamma^* p\rightarrow k'X)=\int dy\, q(y) d\sigma(\gamma^* k\rightarrow k')\ , \tag{1}$$

where $q(y)dy$ is defined to be the number of quarks having momentum fraction between y and $y+dy$, where $y=k\cdot n/p\cdot n$. In terms of scattering matrix elements, we can write the above cross section as

$$d\sigma(\gamma^* p\rightarrow k'X)=\frac{1}{8E_p E_\gamma}|M_{\gamma^* p\rightarrow k'X}|^2 \times(2\pi)^4\delta^4\left[p_\gamma+p-k'-\sum_x k_x\right] \times\prod_x \frac{d^3k_x}{(2\pi)^3 2E_x}\frac{d^3k'}{(2\pi)^3 2E'}\ , \tag{2}$$

$$d\sigma(\gamma^* k\rightarrow k')=\frac{1}{8E_k E_\gamma}|M_{\gamma^* k\rightarrow k'}|^2(2\pi)^4 \times\delta^4(p_\gamma+k-k')\frac{d^3k'}{(2\pi)^3 2E'}\ . \tag{3}$$

Using old-fashioned perturbation theory, the contribution to the matrix element $M_{\gamma^* p\rightarrow k'X}$ in Eq. (2) from a given intermediate state (shown as a dashed line in Fig. 2) is

$$M_{\gamma^* p\rightarrow k'X}=M_{\gamma^* k\rightarrow k'}M_{p\rightarrow kX}\frac{1}{E_x+E_k-E_p}\frac{1}{2E_k}\ . \tag{4}$$

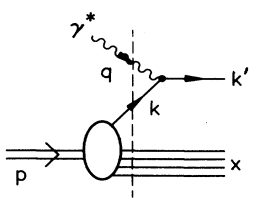

FIG. 2. The leading photon-hadron scattering process to define the quark number density.

Combining these four equations gives the quark number density

$$q(y)dy=\frac{E_k}{E_p}|M_{p\to kX}|^2\left[\frac{1}{E_x+E_k-E_p}\right]^2\left[\frac{1}{2E_k}\right]^2 \times\prod_x\frac{d^3k_x}{(2\pi)^3 2E_x}\ . \tag{5}$$

Because

$$d\sigma(\gamma^*k\to k')=C_\gamma\delta(y-x_B)\ , \tag{6}$$

where $x_B=Q^2/2p\cdot q$, and C_γ depends only on x_B and Q^2, we can write the quark density as

$$q(x_B)=\frac{1}{C_\gamma}d\sigma(\gamma^*p\to k'X)\ , \tag{7}$$

where x_B is the momentum fraction carried by the quark interacting with the virtual photon. We now discuss how fragmentation or fusion of partons perturbs this simple picture.

A. Parton fragmentation or splitting functions

To prepare the way for the parton-parton fusion analysis and as a check of consistency we will first derive the Altarelli-Parisi splitting functions.[6] In the leading-logarithmic approximation, the contribution to the quark-quark splitting function comes from the process shown in Fig. 3. Using old-fashioned perturbation theory and Eq. (7), we obtain the change of quark-number density as

$$dq(x)=\frac{E_l}{E_p}|M_{p\to lX}|^2\left[\frac{1}{E_x+E_l-E_p}\right]^2\left[\frac{1}{2E_l}\right]^2 \times\prod_x\frac{d^3k_x}{(2\pi)^3 2E_x}\frac{E_k}{E_l}|M_{l\to kl'}|^2\left[\frac{1}{E_k+E_{l'}-E_l}\right]^2 \times\left[\frac{1}{2E_k}\right]^2\frac{d^3k_{l'}}{(2\pi)^3 2E_{l'}}\frac{1}{C_\gamma}d\sigma(\gamma^*k\to k')\ . \tag{8}$$

Using Eqs. (5) and (6), we rewrite Eq. (8) as

$$dq(x)=\int dy\ q(y)\left[\frac{\alpha_s}{2\pi}\gamma_{qq}(z)d(\ln l_T^2)dz\right]\delta(zy-x)\ , \tag{9}$$

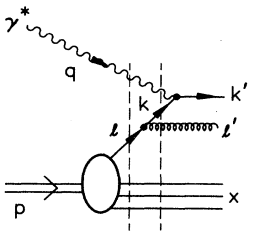

FIG. 3. The next-to-leading photon-hadron scattering process $O(\alpha_s)$ used to calculate the splitting function γ_{qq}.

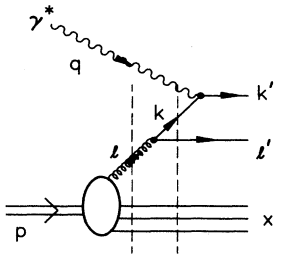

FIG. 4. The next-to-leading singlet photon-hadron scattering process $O(\alpha_s)$ used to calculate the splitting function γ_{qg}, and to define the gluon number density.

where the splitting function $\gamma_{qq}(z)=C_2(R)(1+z^2)/(1-z)$ (Ref. 6). This is a positive contribution causing an increase in $q(x)$—we call it the "gain" part. In terms of the statistical parton evolution picture introduced in Ref. 7, one should include also a negative term (or a "loss" term) into Eq. (9). The complete change of quark density due to the quark splitting process then becomes[7]

$$\frac{dq(x,Q^2)}{d\ln Q^2}=\frac{\alpha_s}{2\pi}\int_0^1 dy\ dz\ q(y,Q^2) \times[\gamma_{qq}(z)\delta(zy-x)-\gamma_{qq}(z)\delta(y-x)]\ . \tag{10}$$

Equation (10) is the same as the well-known valence-quark evolution equation. Physically, in terms of the statistical picture of parton evolution introduced in Ref. 7, the $\delta(zy-x)$ summarizes the gain in $q(x)$ due to quarks of momentum fraction $y>x$ having radiated a gluon of momentum fraction $y-x$. Similarly, the $\delta(y-x)$ contribution summarizes the loss term, identifying all those quarks that had momentum fraction x before radiating a gluon of any momentum fraction less than x.

By computing the leading-logarithmic contribution to the quark density arising from the gluon splitting process in Fig. 4, we obtain the expression for the gluon number density

$$G(y)dy=\frac{E_l}{E_p}|M_{p\to lX}|^2\left[\frac{1}{E_x+E_l-E_p}\right]^2\left[\frac{1}{2E_l}\right]^2 \times\prod_x\frac{d^3k_x}{(2\pi)^3 2E_x}\ . \tag{11}$$

Similarly the gluon-quark splitting function is given by

$$\frac{\alpha_s}{2\pi}\gamma_{qg}(z)d(\ln l_T^2)dz=\frac{E_k}{E_l}|M_{l\to kl'}|^2\left[\frac{1}{E_k+E_{l'}-E_l}\right]^2 \times\left[\frac{1}{2E_k}\right]^2\frac{d^3k_{l'}}{(2\pi)^3 2E_{l'}}\ , \tag{12}$$

which yields the familiar $\gamma_{qg}(z)=\frac{1}{2}[z^2+(1-z)^2]$.

B. Parton fusion functions

Following the same technique, we can derive the parton fusion functions. The quark-gluon fusion process shown in Fig. 5 can change the quark number density as

$$dq(x)=\frac{E_l+E_{l'}}{E_P}|M_{P\to ll'X}|^2\left[\frac{1}{E_x+E_l+E_{l'}-E_P}\right]^2\left[\frac{1}{2E_l}\right]^2\left[\frac{1}{2E_{l'}}\right]^2\prod_x\frac{d^3k_x}{(2\pi)^3 2E_x}$$
$$\times\frac{E_k}{E_l+E_{l'}}|M_{ll'\to k}|^2\left[\frac{1}{E_l+E_{l'}-E_k}\right]^2\left[\frac{1}{2E_k}\right]^2\frac{1}{C_\gamma}d\sigma(\gamma^*k\to k')$$
$$=\int dx_1dx_2T^{(2)}(x_1,x_2,l_T^2)\frac{g^2}{l_T^2}\Gamma_{p_1p_2\to p_3}(x_1,x_2,x_3)\delta(x_3-x)\,, \tag{13}$$

where g is the strong coupling constant, p is the average momentum per nucleon, and P is the momentum of the nucleus (we shall be interested in the fusion of two partons originating in two different nucleons in a nucleus).

The two-parton number density in Eq. (13) is given by

$$T^{(2)}(x_1,x_2,l_T^2)dx_1dx_2$$
$$=\frac{E_l+E_{l'}}{E_P}|M_{P\to ll'X}|^2\left[\frac{1}{E_x+E_l+E_{l'}-E_P}\right]^2$$
$$\times\left[\frac{1}{2E_l}\right]^2\left[\frac{1}{2E_{l'}}\right]^2\prod_x\frac{d^3k_x}{(2\pi)^3 2E_x}\,, \tag{14}$$

where l_T^2 is the transverse momentum of the fusing partons or the scale in such a fusion process as discussed in the following paragraph.

We suppose that the participating partons have undergone normal QCD evolution before the fusion (we refer to these as "fat" partons). For example, as shown in Fig. 6, the quark of number density $q(x_1')$ from one nucleon in a big nucleus evolves first to have number density $q(x_1,Q^2)$, and then fuses with a gluon of number density $G(x_2,Q^2)$ from another nucleon. The transverse size of these fat partons is about $|\Delta b|\sim 1/|Q|$, and the transverse momentum of these fat partons is given by $|l_T|\sim 1/|\Delta b|\sim|Q|$. Therefore, l_T^2 will be of the order of Q^2. Fusions between partons at scales other than Q^2 are incorporated by evolving with the modified evolution equations.[1] Because of this explicit factor of $1/l_T^2$ in Eq. (13) it might appear that this parton fusion disappears as Q^2 increases. However, as discussed in Ref. 3, the modified evolution equations lead finally to only a gradual Q^2 dependence of the fused distributions.

The parton-parton fusion function is given by

$$\frac{g^2}{l_T^2}\Gamma_{p_1p_2\to p_3}(x_1,x_2,x_3)$$
$$=\frac{E_k}{E_l+E_{l'}}|M_{ll'\to k}|^2\times\left[\frac{1}{E_1+E_{l'}-E_k}\right]^2\left[\frac{1}{2E_k}\right]^2, \tag{15}$$

where the parton momenta are chosen to be

$$l=\left[x_1p+\frac{l_T^2}{2x_1p},l_T,x_1p\right],$$
$$l'=\left[x_2p+\frac{l_T^2}{2x_2p},-l_T,x_2p\right],\quad k=(x_3p,0_T,x_3p)\,. \tag{16}$$

If the two partons (p_1 and p_2) are from two different nucleons, as shown in Fig. 6, the two-parton number density can be approximated by[1]

$$T^{(2)}(x_1,x_2,Q^2)=\tfrac{3}{2}R\bar{n}p_1(x_1,Q^2)p_2(x_2,Q^2)\,, \tag{17}$$

where R and $\bar{n}$ are nuclear radius and density, respectively, $\bar{n}=A/(4\pi R^3/3)$, $p_1(x_1,Q^2)$, and $p_2(x_2,Q^2)$ are the parton number densities of the two fusing partons.

The fusion functions are related to the splitting functions. This can be obtained from Eq. (15) and Sec. II A; for a general parton-parton fusion process, shown in Fig. 7, the relation is

$$\Gamma_{p_1p_2\to p_3}(x_1,x_2,x_3)=C_{p_1p_2\to p_3}\left[\frac{x_1x_2}{x_3^2}\right]\gamma_{p_3\to p_1}\left[\frac{x_1}{x_3}\right]$$
$$=C_{p_1p_2\to p_3}\left[\frac{x_1x_2}{x_3^2}\right]\gamma_{p_3\to p_2}\left[\frac{x_2}{x_3}\right], \tag{18}$$

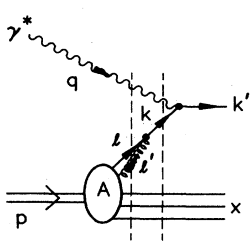

FIG. 5. The leading parton recombination (or fusion) diagram used to define the two-parton number density and to calculate the fusion function $\Gamma_{qg\to q}$.

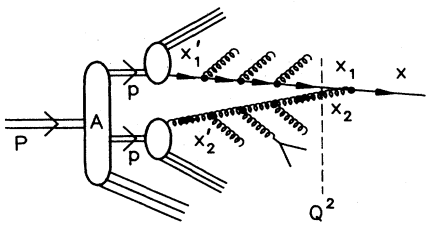

FIG. 6. At a given scale Q^2, the leading fusion contribution to the effective quark distribution occurs between two "fat" partons which have undergone the normal evolution up to this scale.

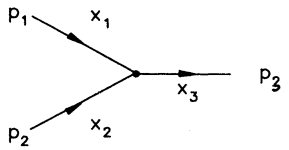

FIG. 7. Momentum assignment for a typical parton-parton fusion process.

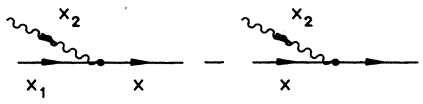

FIG. 8. Quark-gluon fusion diagrams contributing to the $\Delta q_v(x,Q^2)$.

where $C_{p_1p_2\to p_3}$ is a color factor arising due to the difference in the number of initial partons and final partons in the fusion relative to the splitting processes.

In terms of the statistical picture of parton evolution, we obtain the correction to the valence-quark density due to quark-gluon fusion process shown in Fig. 8 as

$$\Delta q_v(x)=2K\int dx_1dx_2q_v(x_1)G(x_2)\times\Gamma_{qg\to q}(x_1,x_2,x_1+x_2)\times[\delta(x-x_1-x_2)-\delta(x-x_1)]\,, \tag{19}$$

where the factor 2 appears because the quark (or gluon) can come from either one of the two nucleons, and $K=9A^{1/3}\alpha_s/(2Q^2r^2)$ where $R=rA^{1/3}$ was used. The fusion function $\Gamma_{qg\to q}(x_1,x_2,x_1+x_2)$ is given by

$$\Gamma_{qg\to q}(x_1,x_2,x_1+x_2)=\frac{1}{6}\frac{x_1x_2}{(x_1+x_2)^2}\frac{1+\left[\dfrac{x_1}{x_1+x_2}\right]^2}{1-\left[\dfrac{x_1}{x_1+x_2}\right]}\,. \tag{20}$$

From Eq. (19), one can verify that this fusion process conserves valence-quark number $\int_0^1 dx\,\Delta q_v(x)=0$.

For the singlet case we must include the quark-antiquark fusion as well as the quark-gluon fusion. Taking into account the processes shown in Figs. 8 and 9, we obtain the modifications to the quark and antiquark number densities as

$$\Delta q_i(x)=2K\left[\int dx_1dx_2q_i(x_1)G(x_2)\Gamma_{qg\to q}(x_1,x_2,x_1+x_2)[\delta(x-x_1-x_2)-\delta(x-x_1)]-\int dx_1dx_2q_i(x_1)\bar{q}_i(x_2)\Gamma_{q\bar{q}\to g}(x_1,x_2,x_1+x_2)\delta(x-x_1)\right], \tag{21}$$

$$\Delta\bar{q}_i(x)=2K\left[\int dx_1dx_2\bar{q}_i(x_1)G(x_2)\Gamma_{qg\to q}(x_1,x_2,x_1+x_2)[\delta(x-x_1-x_2)-\delta(x-x_1)]-\int dx_1dx_2\bar{q}_i(x_1)q_i(x_2)\Gamma_{q\bar{q}\to g}(x_1,x_2,x_1+x_2)\delta(x-x_1)\right], \tag{22}$$

and where the quark-antiquark fusion function is

$$\Gamma_{q\bar{q}\to g}(x_1,x_2,x_1+x_2)=\frac{4}{9}\frac{x_1x_2}{(x_1+x_2)^2}\left[\left[\frac{x_1}{x_1+x_2}\right]^2+\left[1-\frac{x_1}{x_1+x_2}\right]^2\right]. \tag{23}$$

By including the gluon-gluon fusion process of Fig. 10, we obtain the correction to the gluon number density as

$$\Delta G(x)=2K\left[\tfrac{1}{2}\int dx_1dx_2G(x_1)G(x_2)\Gamma_{gg\to g}(x_1,x_2,x_1+x_2)[\delta(x-x_1-x_2)-\delta(x-x_1)-\delta(x-x_2)]+\int dx_1dx_2\sum_i^f q_i(x_1)\bar{q}_i(x_2)\Gamma_{q\bar{q}\to g}(x_1,x_2,x_1+x_2)\delta(x-x_1-x_2)-\int dx_1dx_2G(x_1)\sum_i^f[q_i(x_2)+\bar{q}_i(x_2)]\Gamma_{gq\to q}(x_1,x_2,x_1+x_2)\delta(x-x_1)\right], \tag{24}$$

where the factor $\frac{1}{2}$ in the gluon-gluon fusion contribution is due to the identical particle effect, f is the number of quark flavors and the gluon-gluon and gluon-quark fusion functions are

$$\Gamma_{gg\to g}(x_1,x_2,x_1+x_2)=\frac{3}{4}\frac{x_1x_2}{(x_1+x_2)^2}\left[\frac{z}{1-z}+\frac{1-z}{z}+z(1-z)\right], \tag{25}$$

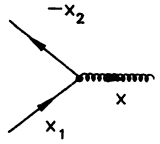

FIG. 9. Quark-antiquark annihilation diagram contributing to the $\Delta q_i(x,Q^2)$.

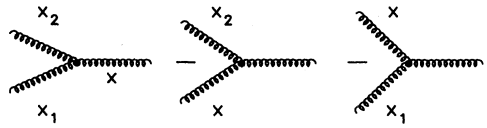

FIG. 10. Gluon-gluon fusion diagrams contributing to the $\Delta G(x,Q^2)$.

with

$$z=x_1/(x_1+x_2)\ ,$$

and

$$\Gamma_{gq\to q}(x_1,x_2,x_1+x_2)=\frac{1}{6}\frac{x_1x_2}{(x_1+x_2)^2}\frac{1+\left[\frac{x_2}{x_1+x_2}\right]^2}{1-\left[\frac{x_2}{x_1+x_2}\right]}\ . \tag{26}$$

If we combine Eqs. (21), (22), and (24), we find

$$\int_0^1 dx\,x\left[\sum_i^f[\Delta q_i(x)+\Delta\bar{q}_i(x)]+\Delta G(x)\right]=0 \tag{27}$$

which verifies that the parton-parton fusion conserves momentum. In addition, as expected, the fusion between gluons alone also conserves momentum. Thus we conclude that the parton-parton fusion, as introduced in this paper, is a self-consistent and a self-contained subprocess of parton evolution.

In the next section we evaluate these parton fusion formulas and obtain the modifications to effective nuclear parton number densities due to the fusion of partons from two neighboring nucleons in a big nucleus.

III. RESULTS

We now proceed to compute the modifications to the structure function and to the gluon distribution in the proton as a result of including parton recombination. We present estimates for the effects of two-parton fusion on the quark and gluon distributions in a nucleus of iron ($A=56$). The picture we have in mind is one where only gluons and sea quarks "leak" from one nucleon into a neighboring nucleon and recombine with the gluons, sea quarks, and valence quarks of that nucleon. We do not consider leakage of valence quarks because their spatial distribution is expected to be limited to about 1 fm. On the other hand, sea quarks and gluons may extend out to several fm.[8]

To investigate the effects of varying the extent to which the sea and the glue leak out of a confined volume, we allow a cutoff distribution $w(x)$:[8a]

$$w(x)=\exp(-\tfrac{1}{2}M^2\langle z^2\rangle x^2)\ . \tag{28}$$

Notice that letting $\langle z^2\rangle^{1/2}\to 0$ corresponds to no cutoff in x while letting $\langle z^2\rangle^{1/2}\to\infty$ reduces $w(x)$ to a spike at $x=0$. We allow $\langle z^2\rangle^{1/2}$ to vary up to 2.4 fm to examine the sensitivity of the results to the cutoff. We find that our result is not sensitive to the value of $\langle z^2\rangle$.

Consider the structure function $F_2(x,Q^2)$ where $F_2(x,Q^2)=\sum_i e_i^2[xq(x,Q^2)+x\bar{q}(x,Q^2)]$. The modification due to leakage of gluons is then given by

$$\Delta F_2(x)=\tfrac{1}{6}K\int_0^x\frac{dx_2}{x_2}x_2G(x_2)w(x_2)\left\{F_2(x-x_2)\left[1+\left[\frac{x-x_2}{2}\right]^2\right]-F_2(x)\left[\frac{x}{x+x_2}\right]\left[1+\left[\frac{x}{x+x_2}\right]^2\right]\right\}$$
$$-\tfrac{1}{6}KF_2(x)\int_x^1\frac{dx_2}{x_2}x_2G(x_2)w(x_2)\left[\frac{x}{x+x_2}\right]\left[1+\left[\frac{x}{x+x_2}\right]^2\right]\ , \tag{29}$$

where we have suppressed the Q^2 dependence of the various parton distributions. Note that the integrand in Eq. (29) is finite as $x_2\to 0$. Similarly the modification due to the sea leaking in and fusing with gluons gives

$$\Delta F_2(x)=\tfrac{1}{6}K\left[\sum_i e_i^2\right]\int_0^x\frac{dx_1}{x_1}x_1G(x_1)\left\{w(x-x_1)(x-x_1)s(x-x_1)\left[1+\left[\frac{x-x_1}{x}\right]^2\right]\right.$$
$$\left.-w(x)xs(x)\left[\frac{x}{x+x_1}\right]\left[1+\left[\frac{x}{x_1+x}\right]^2\right]\right\}$$
$$-\tfrac{1}{6}K\left[\sum_i e_i^2\right]w(x)xs(x)\int_x^1\frac{dx_1}{x_1}x_1G(x_1)\left[\frac{x}{x+x_1}\right]\left[1+\left[\frac{x}{x+x_1}\right]^2\right]\ ; \tag{30}$$

and finally the contribution from the leakage of the sea annihilating with quarks or antiquarks is

$$\Delta F_2(x) = -\tfrac{4}{9}KxF_2(x)\int_0^1 dx_2 w(x_2)x_2 s(x_2)\frac{x^2+x_2^2}{(x+x_2)^4} - \tfrac{4}{9}Kxw(x)xs(x)\int_0^1 dx_1 F_2(x_1)\frac{x^2+x_1^2}{(x+x_1)^4} . \quad (31)$$

In Eqs. (30) and (31) $xs(x)$ is the sea- (anti)quark distribution, assumed to be independent of flavors (we consider only three flavors in our calculations). Of the three contributions, the first is the most important—as seen from Fig. 11. These curves are obtained from Eqs. (30)–(32) taking the Q^2-dependent parton distributions of Martin, Roberts, and Stirling,[9] though the results are not sensitive to the particular set of parton distributions chosen.

For these curves, no cutoff in x was imposed. Next we add the three contributions and vary the cutoff function $w(x)$. In Fig. 12 we show the result of weighting the leaking parton distribution by various cutoff distributions. The results do depend on the cutoff function but not very sensitively. Figure 12 shows that the modification is everywhere positive, though the modification to the valence-quark distribution has a small negative piece at small x—assuring that $\int dx\, \Delta q_v(x)$ is zero. Because of the parton fusion, $\Delta F_2(x)$ does not vanish at $x=1$; indeed the modified nuclear structure function extends to $x=2$. Figure 13 explicitly shows the structure function at large x resulting from parton fusion.

The modifications to the gluon distribution $xG(x,Q^2)$ again have three components. The leakage of gluons [i.e., the first term in Eq. (24)], completely dominates $\Delta xG(x)$. Because of this, *the conservation of momentum between the gluon and quark components is almost separately assured.* In fact, we find that typically only about 0.1% of the momentum is transferred from quarks to gluons in the overall sum of the fusion diagrams. Data are consistent with this prediction.[10] Note that this is a nontrivial result since, *a priori,* momenta could have been transferred from quarks to gluons or vice versa. The near preservation of momentum for each species was implicitly *assumed* in the work of Nikolaev and Zakharov,[11]

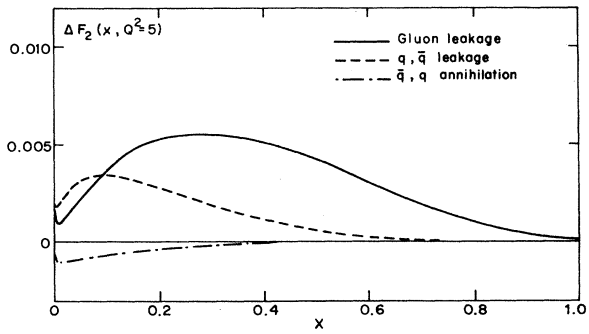

FIG. 11. Contributions to F_2 from the terms displayed in Eqs. (29)–(31).

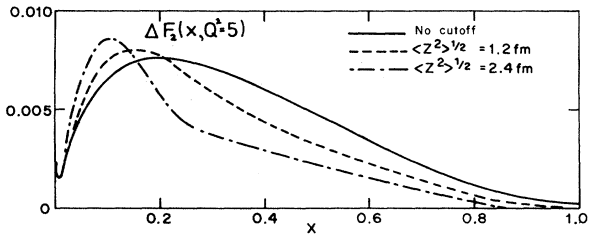

FIG. 12. Effect of imposing different cutoffs in the leakage of partons to recombine with partons in different nucleon.

since their paper preceded QCD and essentially allowed only for charged partons. Thus momentum was trivially conserved within $F_2(x)$ and they necessarily predicted antishadowing to "balance" the shadowed domain. Based on their pion-exchange model, Berger and Coester[12] found that $\int dx\, F_2^A(x,Q^2)$ is essentially independent of A, which implies that the momentum carried by gluons is nearly conserved. Our recombination analysis here justifies that assumption at parton level; moreover we predict a $\Delta xG(x)$ which exhibits shadowing and antishadowing. Figure 14 shows the resulting $\Delta xG(x)$ distribution with a cross-over point around $x=0.06$.

Despite the big difference in the scale of Figs. 11 and 14, the relative changes to the quark and gluon distributions are not dissimilar. Figure 15 shows the ratio of the modified structure function to the free-nucleon structure function at $Q^2=5$ GeV^2 together with the corresponding ratio for $xG(x,Q^2)$. As shown in Fig. 13, parton recombination naturally extends the effective nuclear structure functions to the region where x is larger than 1. The effective nuclear structure function shows a clear antishadowing effect caused by the leading parton recombination processes. The ratio of structure functions shown in Fig. 15 arises when $x \to 1$. The curve shows a feature normally associated with Fermi motion of the nucleons in a nucleus. Our result suggests that the parton recombination

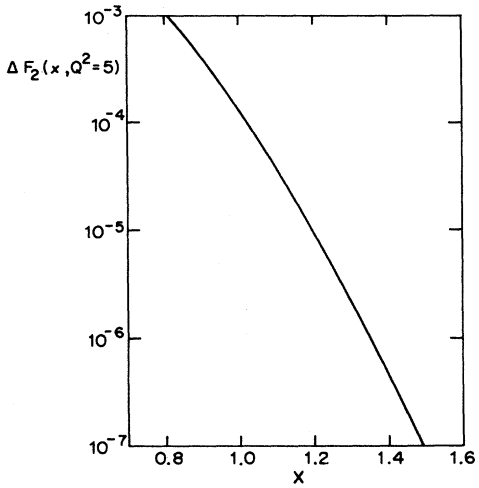

FIG. 13. Structure function at large x resulting from the parton fusions of Eqs. (29)–(31).

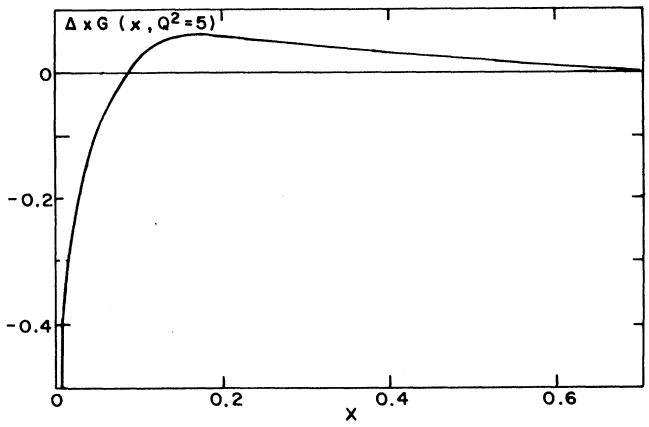

FIG. 14. Parton recombination contribution to the gluon distribution $xG(x,Q^2)$ given by Eq. (24). The dominant term is the gluon-gluon fusion contribution.

between a hard and a soft constituent parton might be an alternate way of describing the Fermi motion effect. However, without completing the calculation of the radiative recombination effect in the large-x region, it is difficult to make a firm conclusion (e.g., on the Q^2 dependence of the $x > 1$ region in this as compared to Fermi-motion descriptions).

However, a complete description of the nuclear structure function in a partonic language could be an amalgam of Q^2 rescaling and parton recombination, both of which result from overlapping of individual nucleons in the nucleus. In that way both the shadowing and antishadowing would merge in a natural phenomenological way.

There are two equivalent ways of regarding the modification of quark and gluon distributions in a bound nucleon compared with those in a free nucleon. In one picture[13] the change arises from the long-distance nuclear forces described in terms of binding potential, Fermi motion, etc., and in the other picture the change results from a modification of the short-distance interaction of the partons—"rescaled QCD" (Ref. 5). Clearly the modification we are discussing here is a natural extra ingredient into the latter description and it may be that parton recombination is an alternate way of describing the modification to the structure function normally associated with Fermi motion of the nucleons in a nucleus.

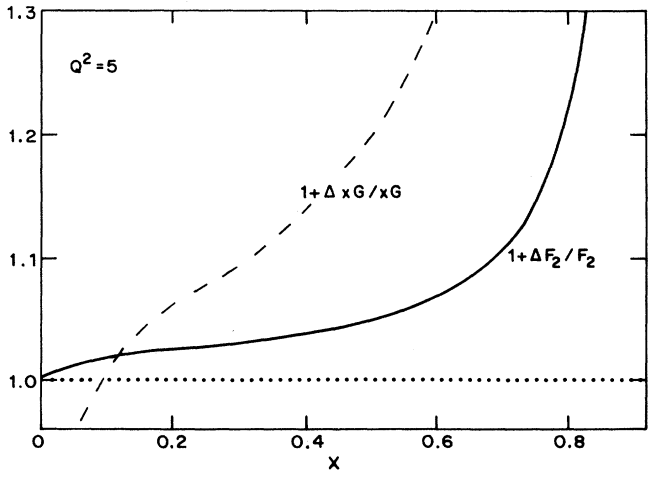

FIG. 15. Ratio of the modified structure function to the nucleon structure function, shown by solid line. The corresponding ratio for the gluon distribution is shown by the dashed line.

IV. NUCLEAR SHADOWING AT SMALL x AND ANTISHADOWING AT LARGE x

In principle, parton recombination involving interactions between two or more partons should be a necessary process in a complete theory of parton evolution. However, the contribution to the leading structure functions from some recombination processes [e.g., that in Fig. 1(b)] is a long-distance effect and factorization enables it to be subsumed within the *input* distributions [as shown in Fig. 1(c)], which are determined by experiment. But as we have noted in the Introduction, such parton recombination processes can play an explicit role in the case of a big nucleus. Typically, there are *two* kinds of recombination processes, depending on whether the hard recombination involves the final-state partons ["radiative recombination," Fig. 16(d)] or not ["initial-state recombination," Fig. 16(b)].

At any chosen Q^2, initial-state recombination gives a direct calculable contribution at that Q^2. The expressions in Sec. III all have a common factor $1/Q^2$ which gives the impression that the effects of parton recombination vanish as the scale Q^2 increases. However, the effective distribution at large Q^2 also receives contributions from radiative recombination diagrams. In Ref. 3 it

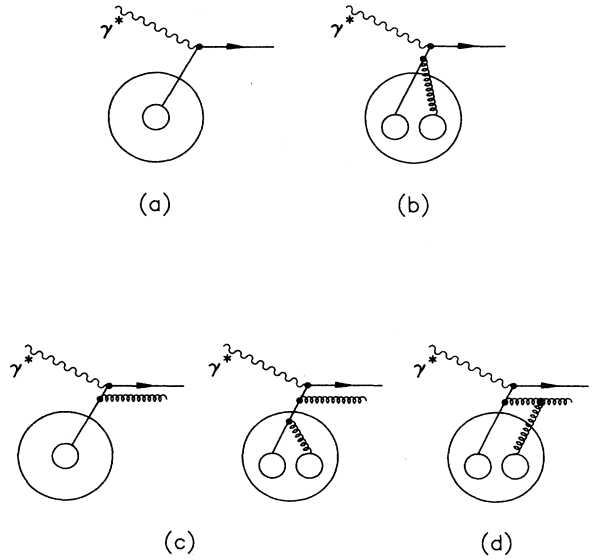

FIG. 16. At a given scale Q^2, the leading contribution (a) and leading fusion correction (b) to the effective nuclear quark distribution; (c) the fusion occurring at a lower scale Q_0^2 effects the distribution at Q^2 through "input" distribution at Q_0^2; (d) the fusion occurring zero between these two scales is included in the modified evolution equations.

was shown that these lead to a modified Altarelli-Parisi equation, one consequence being that the recombination effects die away only slowly, at least in the small-x region; in effect, the nuclear parton distributions at a large Q^2 always retain the memory of recombinations that have occurred at lower values of Q^2.

Thus at any Q^2 both initial and radiative recombination play a role; the net effect is a complicated mix. However, at a low Q^2, where the radiative recombination has not yet really turned on, the initial-state recombination will dominate. Therefore, to estimate the effect of parton recombination in the effective nuclear parton distributions at any given value of x and Q^2, in principle, one should first compute the initial-state recombination to obtain the x dependence of the distributions at a low scale Q_0^2, and then feed these distributions into the evolution equations to get the distributions at the Q^2 of interest.

We now discuss the x dependence of shadowing in the small-x region. In Refs. 1 and 3 the radiative recombination has been found to make a negative contribution to the effective nuclear distributions (thus nuclear shadowing) with only a weak Q^2 dependence, but the x dependences were guessed at on rather general grounds[3] rather than predicted from an underlying theory. But now, having calculated the leading contribution of the initial-state recombination processes, we can estimate the explicit x dependence of the effective nuclear parton distributions at a low Q^2.

We have found a strong gluon shadowing (as shown in Fig. 14) caused by the leading gluon recombination processes. Such strong gluon shadowing will be translated into the effective sea-quark distributions because of parton evolution. We write, for the effective nuclear gluon distribution,

$$xG_A(x,Q^2)=xG(x,Q^2)+\Delta xG(x,Q^2)\ , \tag{32}$$

where $\Delta xG(x,Q^2)$ is the contribution calculated in Secs. II and III of this paper. We display curves at $Q^2=5$ GeV^2 and discuss the choice of this scale later. Similarly, we write, for the quark distributions,

$$xq_A(x,Q^2)=xq(x,Q^2)+\Delta xq(x,Q^2)+\delta xq(x,Q^2)\ , \tag{33}$$

where $\Delta xq(x,Q^2)$ is the contribution from quark-gluon recombination calculated in this paper, but $\delta xq(x,Q^2)$ is the modification due to gluon shadowing and driven by the evolution equations. To get a crude estimate of $\delta xq(x,Q^2)$ we can do the following: In the unmodified Altarelli-Parisi equations in the small-x limit where the dominant graph is the gluon ladder we get solutions for xq and xG in closed form which satisfy

$$xq(x,Q^2)=\frac{1}{4C_2(A)}\frac{\partial xG(x,Q^2)}{\partial \ln(1/x)}=-\frac{x}{12}\frac{\partial xG(x,Q^2)}{\partial x}\ , \tag{34}$$

i.e., the *shape* of the sea-quark distribution at small x is related to the *shape* of the gluon distribution there. Even though ΔxG satisfies a modified form of the Altarelli-Parisi equations, we would still expect a similar relation to hold approximately: i.e.,

$$\delta xq(x,Q^2)\sim-\frac{x}{12}\frac{\partial \Delta xG(x,Q^2)}{\partial x}\ . \tag{35}$$

In Fig. 17, we show the result of using this estimate to compute $R_q=1+(\Delta xq+\delta xq)/xq$ and compare it with $R_G=1+\Delta xG/xG$. Phenomenologically the behavior is consistent with the expectation $R_q<R_G$ (Ref. 13). Consequently, the ratio of F_2^A and F_2 using xq defined in Eq. (33) agrees with the shadowing data.

V. DISCUSSION

In this section, we discuss in some detail the Q^2 scale at which the initial recombination mechanism is the dominant modification. We also justify some approximations involved in our calculation of the leading parton recombination effect, and propose a simple phenomenological program to measure the shadowing effect in the gluon distribution.

In our calculation of parton recombination, we include only processes involving two partons from two different nucleons. In general, the parton recombination between nucleons can involve two or more partons from different nucleons, as long as these partons overlap. However, the short-distance recombination part has higher powers in both α_s and (by dimensional analysis) $1/Q^2$, if more partons are involved. In addition, it is less likely that partons from several different nucleons overlap and hence, we expect that the two-parton recombination involving two different nucleons should be a dominant process to affect the nuclear parton distributions in a region where x is not extremely small. In any event it is natural to study this process first. We have indeed shown in this paper that the two-parton recombination (or fusion) process makes an important modification of the effective nuclear parton distributions in both the small-x and large-x re-

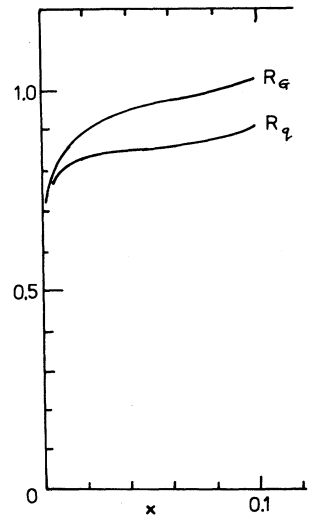

FIG. 17. The ratio of the effective nuclear and nucleon parton distributions at $Q^2=5$ GeV^2. The solid line is $R_G=1+\Delta xG/xG$ given in Eq. (32), and the dashed line is $R_q=1+\Delta xq/xq+\delta xq/xq$ given in Eq. (33).

gions. Moreover, the two-parton recombination process itself is a self-consistent process, preserving the basic conservation laws—valence-quark-number conservation and momentum conservation.

One might argue that the effect of the initial-state recombination should be subsumed within the effective *nuclear* input parton distributions as is conventionally the case with nucleons. However, a nucleus is not just a "big" nucleon; it has its own unique substructure. The individually confined nucleons in a nucleus have their own domains. They are bound to form the nucleus by the *effective* nuclear force acting between them. When one probes a nucleus at a low momentum transfer, the quarks and gluons appear to be confined within individual pions and nucleons. At a very high momentum transfer (i.e., in the asymptotic phase where perturbative QCD is valid), the sea and gluons may spread over a couple of fm (Ref. 5). So the nucleus appears rather different at the parton level. The valence quarks of each nucleon are *still* in that nucleon's own domain, while the gluons and sea quarks from different nucleons may overlap with each other. Because of the overlapping, the parton distributions in a nucleus will not be equal to the simple sum of the parton distributions of individual nucleons. Knowing the parton distributions of an individually confined nucleon, we may calculate the recombination effect between partons from different nucleons, and thus estimate the effective nuclear parton distributions and learn *directly* the effect of parton recombination.

At any Q^2 the net recombination involves initial-state recombination of parton distributions appropriate to that Q^2, plus the effect of radiative recombinations of distributions appropriate to lower values of Q^2. The initial-state recombination will give a better approximation to the total if Q^2 is small; for large Q^2 it is most efficient to compute the effects of initial recombinations alone at some small Q_0^2 and then evolve the resulting nuclear distribution as in Refs. 1 and 3.

If one is eventually to make sensible phenomenology with this formalism, it will be necessary to have some prior knowledge of Q_0^2. At present this is an undetermined boundary condition for us; $Q_0^2=5$ GeV^2 seems to work well. In the absence of a complete theory, and to aid insight into possible phenomenological exploitation of these ideas, it may be useful to exhibit and discuss the Q^2 dependences of the initial recombinations.

In Fig. 18 we show the qualitative trend of $x\Delta q_v$. At $x>0.3$ the Q^2 factor [Eq. (19)] kills the recombination by a factor of 4 ($Q^2=5$–20 GeV^2); the QCD evolution of the intrinsic input $q_v(x,Q^2)$ is responsible for suppressing Δq_v ($x>0.5$) by a further 25% and also causes a net shift to smaller x values.

The value of x where $\Delta q_v(x)$ changes sign (x_5 in Ref. 14) is a sensitive function of the shapes of the input distributions. For example, in the limit that $xq_v(x)\to\delta(x)$ then Eq. (19) yields

$$x\Delta q_v(x>0)=\tfrac{1}{3}KG(x)\ , \tag{36}$$

hence, positive for all nonzero x. So we see here the natural tendency for $x_5\to 0$ as the input quark distributions peak at smaller x (e.g., higher Q^2).

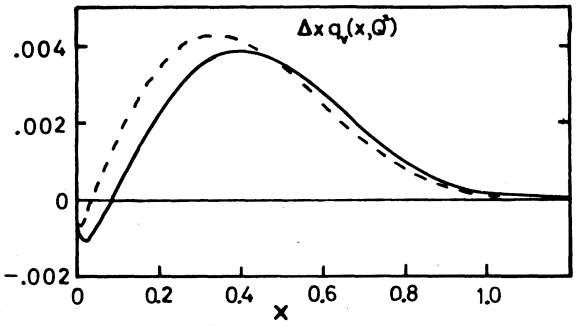

FIG. 18. The qualitative trend of $\Delta xq_v(x,Q^2)$ at $Q^2=5$ GeV^2 (solid line), and at $Q^2=20$ GeV^2 (dashed line).

This property causes initial recombinations involving the sharply peaked $q\bar{q}$ sea distributions to cause antishadowing at small x. This is responsible for the very different types of behavior that ensue for $\Delta F_2(x)$ at small x (Fig. 19), as Q^2 varies.

At $Q^2=20$ GeV^2 the contribution from $x\Delta q_v(x)$ is antishadowed for $x\gtrsim 0.03$ (Fig. 18). In addition the sharply peaked sea distributions are important at this large Q^2 and amplify this antishadowing causing the positive spike in $\Delta F_2(x\to 0)$.

Compare this with the initial-state recombination for $\Delta F_2(x,Q^2=5\ \text{GeV}^2)$. The contribution from $x\Delta q_v$ in Fig. 18 is shadowed for $x<0.2$ now. Even at this small value of Q^2 the sea, albeit reduced in importance, tends to cancel this suppression; x_5 is pulled down to 0.05 but some shadowing remains for $x<0.05$. If we could devolve in Q^2 to the point where no $q\bar{q}$ sea were present, then $\Delta F_2(x)$ would behave as $x\Delta q_v(x)$ in Fig. 18, with x_5 tending to the value of x where $q_v(x)$ maximizes.

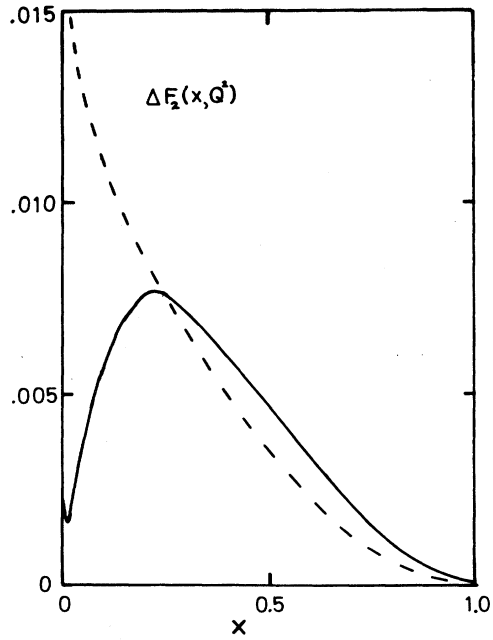

FIG. 19. $\Delta F_2(x,Q^2)$ as a function of x at $Q^2=5$ GeV^2 (solid line), and at $Q^2=20$ GeV^2 (dashed line).

In the above we have taken no account of radiative recombination. This can distort the large Q^2 results considerably and cause retention at high Q^2 of the shadowing and antishadowing structure manifest at *low* Q^2 in Fig. 19. A feeling for how this comes about can be gained by concentrating on the three-gluon vertex which plays an important role in the evolution especially at small x (at large x the shape of ΔF_2 is fairly stable as we have seen).

The effective nuclear gluon distribution is strongly shadowed as $x \to 0$ as seen in Fig. 14. Indeed, from Eq. (24), if $xG(x) = \text{const}$ as $x \to 0$ then

$$\Delta G(x \to 0) \simeq -[xG(x)]^2 . \tag{37}$$

Insofar as the $q\bar{q}$ sea is evolved from gluons at lower Q^2, then $\Delta G(x \to 0)$, being negative, will evolve into a negative (i.e., shadowed) contribution to the effective sea distribution in the nucleus. Moreover, Eq. (37) shows that $\Delta G(x \to 0)$ is in proportion to the *square* of the input gluon distributions (it is, after all, a fusion of *two* input gluon distributions) and so the shadowing of $q\bar{q}$ coming from the evolution of ΔG dominates over the antishadowing of the initial-state recombination (dotted curve in Fig. 19). The result qualitatively is to retain the structure of $\Delta F_2(x)$ revealed at low Q^2 (solid curve in Fig. 19). A complete calculation of radiative recombination at small x given in Refs. 1 and 3 actually confirms this conclusion—the recombination effect has a very weak Q^2 dependence.

Deep-inelastic lepton-nucleus scattering and hadron-nucleus Drell-Yan experiments provide measurements of the shadowing for quark and antiquark distributions; we now propose a simple program to measure the shadowing of the gluon distribution by means of hadronic J/ψ production on different nuclear targets. In experiment E537 at Fermilab, the nuclear dependence of the J/ψ production has been measured as a function of x_2 (Ref. 15). The experiment covers values of x_2 from 0.18 down to about 0.05, and shows clear shadowing over this entire region, as shown in Fig. 20. In particular, it shows very *strong* shadowing even at $x_2 \sim 0.18$. In our picture of nuclear shadowing, partons are expected overlap and to generate shadowing only when $x_2 \lesssim 0.1$–0.2 (Refs. 3, 14, and 16); we do not expect strong shadowing for $x_2 \sim 0.18$. However, the shadowing observed in J/ψ production is a consequence of *two* different effects, only one of which is the parton level shadowing that we have been discussing here. The other is hadronic shadowing due to the "color screening" or "color transparency"[17] when the $c\bar{c}$ pair with a small value of χ_F, produced by a hard short-distance parton level interaction (e.g., gg fusion) subsequently passes through the nuclear medium on its way to form the J/ψ.

In order to measure the shadowing of the intrinsic gluon distribution—the parton level shadowing—we must first separate the hadronic shadowing from the data. We propose the following procedure. Because the hadronic shadowing is caused by interactions between the produced $c\bar{c}$ pair and the nuclear medium, it should depend on x_F rather than a specific value of x_2. In contrast, the parton level shadowing due to parton recombination depends on the explicit value of x_2; and the shadowing is small if $x_2 \gtrsim 0.1$. Knowing these facts, one can measure the nuclear shadowing of gluon distributions *without* really dealing with the more complicated hadronic shadowing problem.

(1) Measure the shadowing in J/ψ production at a relative low energy ($x_2 \gtrsim 0.1$), and parametrize the x_F dependence of the observed nuclear shadowing. Our analysis suggests that this shadowing phenomenon should include only hadronic shadowing.

(2) Repeat the experiment at a higher energy (x_2 can now be less than 0.1), and subtract the hadronic shadowing effect (the x_F parametrization obtained in the first step) from the data.

(3) Whatever shadowing remains after the subtraction is the parton level shadowing: namely, that of the gluon distributions if the dominant production mechanism of the $c\bar{c}$ gluon fusion. In our simple program we have used the experimental fact that the hadronic shadowing (or the ratio shown in Fig. 20) is mostly sensitive to x_F, not to the colliding energy.

In conclusion, we have shown how the qualitative features of the recombination mechanism can be understood, but we are still some way from implementing a complete phenomenology. We have no satisfactory theory for the input Q_0^2 at which the initial-state recombination dominates and from which the evolution begins. The pleasing description of the x dependence of shadowing, rooted in QCD and exhibited in Fig. 14, is indeed an advance, modulo these caveats. However, the main thrust of this paper has been to investigate recombination and to understand its qualitative behavior. The results suggest that parton recombination may be the most important mechanism for modifying the structure functions at low x, by generating shadowing, and at large x. The

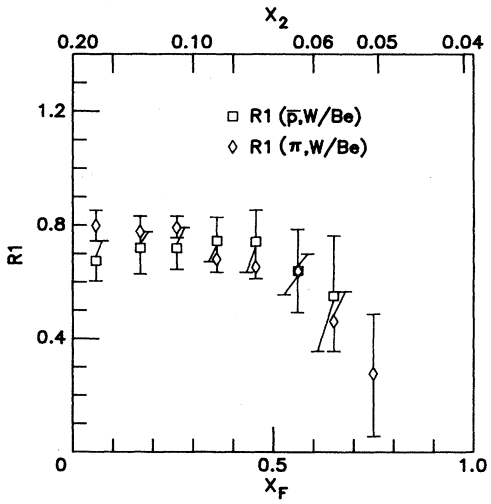

FIG. 20. The ratios of hadronic J/ψ production (Ref. 15) ($A^{-1}d\sigma^A/dx_F$) for $\pi^- W$ to π^-Be, and for $\pi^- W$ to π^-Cu as a function of x_F.

physical picture of boosting fast partons at the expense of wee ones seems likely to survive more detailed investigation. Recombination seems to have little relevance to the intermediate range of x, at least if the EMC data on F_2 are a guide. However, we know that the recombination diagrams are only one part of the set of QCD diagrams. The effects of rescaling the more familiar radiative diagrams are well known[5,18] and by themselves make a reasonably successful description of that region of x. It would be logically consistent to combine these and form a complete QCD-based description of effective nuclear structure functions in terms of short-distance quark and gluon interactions.

ACKNOWLEDGMENTS

One of us (F.C.) wishes to thank J. F. Owens for useful conversations. Another of us (J.Q.) is grateful to E. L. Berger and A. H. Mueller for helpful discussions.

[1]A. H. Mueller and J. Qiu, Nucl. Phys. **B268**, 427 (1986).

[2]L. V. Gribov, E. M. Levin, and M. G. Ryskin, Nucl. Phys. **B188**, 555 (1981); Phys. Rep. **100**, 1 (1983).

[3]J. Qiu, Nucl. Phys. **B291**, 746 (1987); E. L. Berger and J. Qiu, in *Proceedings of the Topical Conference on Nuclear Chromodynamics,* Argonne, Illinois, 1988, edited by J. Qiu and D. Sivers (World Scientific, Singapore, 1988).

[4]K. P. Das and R. C. Hwa, Phys. Lett. **68B**, 459 (1977).

[5]F. E. Close, R. G. Roberts, and G. G. Ross, Nucl. Phys. **B296**, 582 (1988).

[6]G. Altarelli and G. Parisi, Nucl. Phys. **B126**, 298 (1977).

[7]J. C. Collins and J. Qiu, Phys. Rev. D **39**, 1398 (1989); L. N. Lipatov, Yad. Fiz. **20**, 181 (1974) [Sov. J. Nucl. Phys. **20**, 94 (1975)].

[8]C. H. Llewellyn Smith, Nucl. Phys. **A434**, 350 (1985).

[8a]The cutoff distribution $w(x)$ is related to a light-cone correlation $C(z)$ (Ref. 8) by $w(x)=\int dx\cos(Mzx)C(z)$. To get Eq. (28), we choose $C(z)$ to be $(2\beta/\sqrt{\pi})\exp(-\beta^2z^2)$ where $\langle z^2\rangle^{1/2}=(\sqrt{2}\beta)^{-1}$.

[9]A. D. Martin, R. G. Roberts, and W. J. Stirling, Phys. Rev. D **37**, 1161 (1988).

[10]B. Povh, proceedings of American Physical Society meeting at Santa Fe, New Mexico, 1988 (unpublished).

[11]N. N. Nikolaev and V. I. Zakharov, Phys, Lett. **55B**, 397 (1975).

[12]E. L. Berger and F. Coester, Annu. Rev. Nucl. Part. Sci. **37**, 463 (1987); Phys. Rev. D **32**, 1071 (1985).

[13]C. H. Llewellyn Smith, Phys. Lett. **128B**, 107 (1983); M. Ericson and A. W. Thomas, *ibid.* **128B**, 112 (1983); E. L. Berger, F. Coester, and R. B. Wiringa, Phys. Rev. D **29**, 398 (1984).

[14]F. E. Close and R. G. Roberts, Phys. Lett. B **213**, 91 (1988).

[15]S. Katsanevas *et al.*, Phys. Rev. Lett. **60**, 2121 (1988).

[16]E. L. Berger and J. Qiu, Phys. Lett. B **206**, 141 (1988).

[17]S. J. Brodsky and A. H. Mueller, Phys. Lett. B **206**, 685 (1988); A. H. Mueller, Columbia University Report No. CU-TP-412 (unpublished).

[18]R. Jaffe, F. E. Close, R. G. Roberts, and G. G. Ross, Phys. Rev. D **31**, 1004 (1985).